Chemical Engineering and Technology, Volume 44, Issue 4, April 2021, pp. 1-8
DOI: 10.1002/ceat.202000590

Production of high-purity hydrogen and layered doubled hydroxide by the hydrolysis of Mg-Al alloys

Tong Zheng[1], Jingqi Zhang[1], Yang Tang[2], Pingyu Wan[2], Qipeng Yuan[3], Hanjun Hu[4], Frederic Coulon[5], Qing Hu[4], Xiao Jin Yang[1,*]

[1] Beijing Key Laboratory of Membrane Science and Technology, College of Chemical Engineering, Beijing University of Chemical Technology, 100029, Beijing, China.

[2] College of Chemistry, Beijing University of Chemical Technology, 100029, Beijing, China.

[3] Department of Pharmaceutical Engineering, Beijing University of Chemical Technology, Beijing, 100029, China.

[4] School of Environmental Science and Engineering, Southern University of Science and Technology, Shenzhen, 518055, China.

[5] School of Water, Energy and Environment, Cranfield University, Cranfield MK43 0AL, UK.

*Correspondence: Xiao Jin Yang (E-mail: yangxj@mail.buct.edu.cn.), Beijing Key Laboratory of Membrane Science and Technology, College of Chemical Engineering, Beijing University of Chemical Technology, 100029, Beijing, China.

Abstract

Hydrogen is becoming important clean energy and layered doubled hydroxide (LDH) is of great interest to many applications, including water treatment, environmental remediation and chemical catalysis. Here, we report production of high-purity hydrogen and LDH by the hydrolysis of Mg-Al alloys. The effects of initial pH 1-9, reaction temperature 25-70 °C, reaction time 9 h-15 d and alloy's Mg/Al mass ratio (30-70% Al) are investigated on the rate of hydrogen generation and the purity of LDH. The solid hydrolysis products are characterized using inductively coupled plasma optical emission spectrometry, X-ray diffraction, scanning electron microscope, transmission electron microscope, fourier transform infrared spectrometer, thermal gravimetric analyzer, mapping and particle size distribution analyzer. The initial rate of hydrogen generation increases with decreasing initial pH and increasing reaction temperature and Mg/Al ratio while the purity of LDH increases with Mg/Al ratio, reaction temperature and time. Mg-Al alloys with 40-50% Al generate the highest yield of hydrogen and the 30% Al alloy produces pure and well-crystallized LDH with an average particle size of 217 nm, crystallite size of 16 nm and a specific surface area of 55 m^2/g. This study may provide a new, green and sustainable approach for storage of hydrogen and material of water treatment.

Keywords: Alloys; Hydrogen production; Layered doubled hydroxide; Sustainable development

1. Introduction

Clean energy and clean water are essential for sustainable societies while the sustainability of our world has faced a great challenge by environmental pollution, due primarily to consumption of fossil fuels [1]. Hydrogen energy was proposed to address the pitfalls of fossil energy in 1970s [2] but the safety concern of transportation and storage of hydrogen has been one of the key issues for its use [3]. Therefore, on-board generation of hydrogen is required in many applications (e.g. closed vessels, aircraft, space ship and submarine, etc.) [4-6].

On-board hydrogen generation by the hydrolysis of Al metal has attracted great attention due to its rapid and simple process [7, 8]. The cost of on-board hydrogen production by Al metal hydrolysis is much lower (US$3/kg) than that of $NaBH_4$ decomposition method [9] while the hydrolysis byproduct $Al(OH)_3$ can be recycled through Hall-Heroult process [10]. Most importantly, Al has relatively high hydrogen production capacity (0.11 kg H_2 per kg Al) [11]. Nevertheless, the dense film of alumina on the surface of Al metal protects Al metal underneath and the byproduct on the surface further inhibits hydrolysis reaction [12]. To overcome this problem, high NaOH concentrations [13, 14] and alloying Al with other electrochemically noble metals (Ga, Li, Bi), common transition metals (Fe and Cu) [9, 12, 15-19] and alkaline earth metals (Ca and Mg) [20-22] are employed to promote the hydrolysis reaction. However, the formation of $Al(OH)_3$ and $Mg(OH)_2$ films hinders hydrolysis reaction [1, 23] and the recycled use of solid hydrolysis products could be problematic due to doped metals. The latter problem has been ignored in the literature and clearly, this practice does not fit with the concept of green and sustainable development.

Water contamination has become a global concern and the development of new materials for water remediation and purification is a core attention of water treatment research and industry [24]. Of various water treatment materials, layered doubled hydroxide (LDH) is an emerging material due to its high capacity of adsorption and ion-exchange [25]. LDH has also been widely used in synthesis, catalysis, drug delivery, imaging, targeting, bio-sensing and anti-microbial formulation [26, 27]. In many applications, relatively pure LDH is required, for instance, sodium and nitrate are potential poisons in LDH catalysts [28, 29]. The most common method for LDH synthesis is co-precipitation of Mg and Al salt solutions (nitrate or chloride) in sodium alkaline solutions [30, 31] and multiple washes using a large amount of water are required to remove impurities. Even though, it is difficult to obtain pure (e.g. anions-free) LDH [32] and new methods of synthesizing high-purity LDH are highly demanded [33, 34].

In the co-precipitation process for LDH synthesis using Mg and Al nitrate or chloride as divalent and trivalent metal sources, the solution pH 9-10 and Mg/Al molar concentration ratios of 2-4 are important

Published by Wiley. This is the Author Accepted Manuscript issued with: Creative Commons Attribution Non-Commercial License (CC:BY:NC 4.0).
The final published version (version of record) is available online at DOI:10.1002/ceat.202000590. Please refer to any applicable publisher terms of use.

for producing well-structured and crystalized LDH. These conditions can be readily controlled and/or maintained in the co-precipitation process [35, 36]. However, it is difficult to achieve similar conditions for LDH formation if Mg and Al ions are supplied by the hydrolysis of Mg and Al alloys because the hydrolysis rate of the alloys is highly dependent on the alloy's and solution compositions. In the hydrolysis of Al alloys (Al-Ca, Al-Fe, Al-Bi, Al-Mg), the hydrolysis rate is determined by the operating condition (pH and reaction temperature) and alloy's composition (Al and alloyed metal concentration) [17, 37]. Increasing alloyed metal concentration decreased hydrogen generation rate [11, 38] and hydrolysis byproducts metal hydroxides hampered hydrogen generation [17, 22, 23]. Obviously, it was a challenge to generate hydrogen at desired rates and yields, meanwhile produce highly pure, well-structured LDH by the hydrolysis of Mg-Al alloys. This study was aimed to investigate production of hydrogen and high-purity LDH from the hydrolysis of Mg-Al alloys by examining the effect of alloy's composition (Mg/Al ratio), initial pH, reaction temperature and time and to compare the characteristics of Mg-Al alloy hydrolysis LDH with conventional co-precipitation and commercially available LDH.

2 Experimental

2.1 Preparation of Mg-Al alloys

Mg-Al alloys were prepared by melting pure Mg and Al powders (at different mass ratios 70/30, 60/40, 50/50/ 40/60, 30/70) using MgO crucible in a vacuum electric furnace (SGM.VB6/16, Sigma Furnace Industry, China) at a vacuum pressure of <5 Pa. The temperature of the furnace was increased from room temperature to 750 ˚C at a rate of 70 ˚C 10 min^{-1} and was maintained for 30 min. The furnace was then cooled to room temperature and the Mg-Al alloy ingot was crushed into powders of 80-200 meshes.

2.2 LDH synthesis by co-precipitation

The synthesis of MgAl-LDH by direct co-precipitation [39] is briefly described as follows. Aqueous solutions of $MgCl_2$ (0.625 M, 100 mL) and $AlCl_3$ (0.25 M, 100 mL) were prepared by dissolving $MgCl_2{\cdot}6H_2O$ and $AlCl_3{\cdot}6H_2O$ in deionized water. These two solutions and NaOH solution (0.5 M) were slowly added into 50 mL deionized water in a three-necked flask in a water bath (70 °C) under stirring. The pH of the solution was controlled at 9-10 by the addition of NaOH solution and the resulting suspension was stirred under nitrogen atmosphere for 40 h. The precipitate was filtered, washed with deionized water to neutral pH and then dried under vacuum at 80 °C about 24 h.

2.3 The hydrolysis of Mg-Al alloys

1.5 g Mg-Al alloy was loaded in the 250 mL glass bottle, which was put into water bath kettle. The volume of hydrogen was measured by the drainage method using measuring cylinder. Solutions of different pH values were pumped into the glass bottle through peristaltic pump. Solutions were stirred by a magneton (200 rpm) until the alloy reacted completely. Then the suspension were centrifuged, washed and dried in the vacuum drying oven at 80 °C about 24 h.

2.4 Characterization

X-ray diffraction (XRD) pattern of samples were recorded using Ultima IV (185 mm) at 40 kV/40 mA with Cu Kα radiation (λ=1.5406 Å). The morphology and size of samples were determined by scanning electron microscopy (SEM, HITACHI S-4700) and laser particle size analyzer (Zetersizer Nano ZS980). Mg ang Al contents in the alloys were measured by inductively coupled plasma optical emission spectrometry (ICP-OES, Thermo Fisher, iCAP 6000) after digestion using HNO_3. Thermogravimetric analysis (TGA) and differential thermal analysis (DTA) of Mg-Al LDH were performed using Thermo-Analyzer System (NETZSCH STA 449F3) in the temperature range of 25-800 °C at a heating rate of 10 °C/min in flowing nitrogen gas. Transmission electron micrographs (TEM) were recorded on an JEM2200FS TEM instrument. Fourier transform infrared spectroscopy (FT-IR) was conducted with IRTracer-100 to analyze the chemical bondings of the samples and surface functional groups within the wavenumber range from 400 to 4000

cm^{-1}. The Brunauer–Emmett–Teller (BET) specific surface area measurement were investigated using a nitrogen adsorption device QuadraSorb SI.

3. Results and discussion

The parameters affecting hydrogen generation by the hydrolysis of Al alloys (Al-Mg, Al-Ca, Al-Fe) include alloy's composition, reaction temperature, hydrolysis solution conditions [11, 17, 40]. Fig. 1 shows the rate of hydrogen generation and XRD characterization of hydrolysis products at different initial pH, reaction temperature and alloy's composition. Hydrogen generation increases with decreasing initial pH (Fig. 1a) and hydrogen yield is between 41%-66% in the hydrolysis time of 60 h. Hydrogen generation rises sharply in 1 h and then slows down at initial pH 1.1 while it experiences an induction stage and then accelerates at initial pH 2.9-9.14. This phenomenon is likely due to the rapid dissolution of protective layer of metal oxides and fast reaction of fresh alloy with hydrogen ions at pH 1.1. The dissolution of metal oxides layer on the alloy's surface is much slower at initial pH 2.9-9.14 and hydrogen generation increases when the protection layer is dissolved. The hydrolysis products are mixtures of $Al(OH)_3$ and LDH and the content of $Al(OH)_3$ increases with increasing pH (Fig. 1b). LDH was characterized by typical basal peaks 003, 006 and 009 in XRD [41, 42].

Hydrogen generation increases with increasing reaction temperature between 25 and 55 °C and there are no significant differences between 55 °C and 70 °C (Fig. 1c). An induction period of 15 h is observed at 25 °C and this is caused by slow dissolution of metal oxides layer. Both LDH and $Al(OH)_3$ are produced and the amount of LDH increases with increasing reaction temperature (Fig. 1d). It seems difficult to see the trend of hydrogen generation for different Mg/Al ratios (Fig. 1e) while the quantity of LDH increases with increasing Mg/Al ratio and pure LDH is obtained from the hydrolysis product of Mg-Al30 (Fig. 1f). Nevertheless, initial rates of hydrogen generation in the first period of 5 h increase with increasing alloy's Mg/Al ratio from 30/70 to 70/30. This indicates that Mg makes higher contribution to hydrogen generation in the initial reaction period. After 40 h reaction, hydrogen generation is almost leveled off for all types of the alloys and Mg-Al60 and Mg-Al50 produce almost the same volume of hydrogen (1300 mL) while the total volume of hydrogen from Mg-Al70, Mg-Al40 and Mg-Al30 is similar (902-976 mL). Hydrogen yield from Mg-Al50 and Mg-Al60 is approximately 74% and 69% while it is 47-58% for Mg-Al70, Mg-Al40 and Mg-Al30. LDH coatings have been developed to improve the corrosion resistance for Mg alloys [43] and Al alloys [44]. Therefore, the relatively low yields of hydrogen obtained here were likely caused by surface passivation of Mg-Al alloys by LDH.

Escobar-Alarcón et al. [22] reported hydrogen production by ultrasound assisted liquid laser ablation of Al, Mg and Mg-Al alloys (Mg-Al32, Mg-Al82, Mg-Al92) in water and found that hydrogen production increased with increasing alloy's Al concentration. Their Mg-Al32 alloy was mixtures of Mg phase and $Mg_{17}Al_{12}$ and they also observed surface passivation of Al-Mg alloys. $Mg_{17}Al_{12}$ was considered potential for hydrogen storage [45, 46] but it is relatively inert to split water as compared to Al or Mg alone [21]. The major component of Mg-Al60 and Mg-Al70 alloys investigated in this work is Mg_2Al_3 and that of Mg-Al50, Mg-Al40 and Mg-Al30 is $Mg_{17}Al_{12}$. Zou et al. [47] observed that the hydrolysis of Mg/Al 70/30 alloy doped with 3% Co metal and 2% Bi metal in seawater presented 97.2% hydrogen yield and that the hydrolysis products were mixtures of $Mg(OH)_2$ and Al and Mg-based amorphous compounds. In this study, we observed LDH coated alloy composites, which may be of great interest to chemical catalysis and water treatment.

Fig. 2 shows the concentration of Al and Mg ions and pH variation of the hydrolysis solution and SEM and BET characterization of the hydrolysis products by Mg-Al alloys. Both Al and Mg ion concentrations increase rapidly within 10 h and then decrease sharply. The maximum concentration of Al ion decreases significantly with the increase of Mg/Al ratio from 764 mg/L (Mg-Al70) to 36 mg/L (Mg-Al30) while the maximum Mg ion concentration is similar at 660-700 mg/L for all types of the alloys. The pH of the solution increases from pH 1 to pH 7-9 and then remains almost unchanged. The time to reach the turning point

of the pH is 24 h for Mg-Al70 and decreases with the decrease of Mg/Al ratios. The morphology of the product is a typical LDH structure of "rose-like" and the BET specific surface area is between 37 and 55 m^2/g.

In the co-precipitation process, a reaction time of 8 h and temperature of 90 °C are required to produce well-structured LDH [48]. The XRD characterization of hydrolysis product from Mg-Al30 at the temperature of 25 °C and 70 °C is shown in Fig. 3. A reaction time of 50 h is required to produce relatively pure LDH from Mg-Al30 at 25 °C while a reaction time of 9 h is sufficient to generate a well-crystallized and pure LDH product at 70 °C. The LDH product from Mg-Al30 (initial pH 1, HCl; 70 °C and 40 h) was characterized by SEM (Fig. 4a), TEM (Fig. 4b, c), mapping (Fig. 4d), FT-IR (Fig. 5a), TG-DTA (Fig. 5b) and Particle size (Fig. 5c). The mapping image indicates that interlamellar Cl exists in the MgAl LDH. The broad band at 3473 cm^{-1} in the FT-IR is attributed to stretching vibration of hydroxyl groups and water molecules [49] and the band at 1632 cm^{-1} is assigned to the bending vibration of interlayer water molecules [39, 49, 50]. The peak at 1375 cm^{-1} is associated with CO_3^{2-} in the interlayer and the sharp bands approximately at 679 cm^{-1} and 447 cm^{-1} are interpreted as the lattice vibrations of Al-O and Mg-O [39, 41, 50, 51]. The TG-DTA curve has three decomposition steps and the first step from 70 °C to 190 °C is to eliminate interlayer water molecules [52]. Dehydroxylation of the brucite-like octahedral layer is observed in the second step between 190 °C and 390 °C [53]. Finally, CO_3^{2-} loss is observed in the temperature range of 390 °C-580 °C [52]. The weight loss in these three steps is 7.56%, 18.24% and 11.86%, respectively. The chemical formula of LDH is determined to be $[Mg_{18}Al_7(OH)_{50}][Cl_3(CO_3)_2 \cdot 5H_2O]$.

The characterization of Mg-Al alloy hydrolysis, commercial and co-precipitation LDH samples by XRD, SEM and BET is shown in Table. 1 and Fig. 6. The Mg-Al alloy hydrolysis product presents typical characteristics of LDH and more importantly it possesses significantly larger specific surface area than those obtained by conventional co-precipitation process. It is likely that hydrogen generation is conducive to enhance surface area of the hydrolysis product and this hypothesis is under investigation. It should be noted that condition). Recently, Sotiles et al. [25] reported for the first time that LDH can be considered cation Mg-Al alloy hydrolysis LDH can be free of alkali metals, anion ions or both (depending on the hydrolysis exchangers, opening new avenues for scientific and industrial applications. Therefore, it would be of interest to investigate cation exchange performance of Mg-Al alloy hydrolysis LDH for potential applications.

4. Conclusion

The hydrolysis of Mg-Al alloys at different initial pH 1-9 produces hydrogen and layered doubled hydroxides (LDH). Hydrogen generation rate increases with increasing reaction temperature and the alloy's Mg/Al ratio. The hydrolysis products can be relatively pure LDH free of alkaline metals and anions or nanocomposites of LDH, $Al(OH)_3$ and etched alloy particles by using suitable Mg/Al ratio alloys and controlling the time of hydrolysis. The hydrolysis of Mg-Al alloy with a Mg/Al mass ratio of 70/30 in deionized water and dilute HCl solutions produces alkaline metal- and/or anion-free, pure LDH phase. Mg -Al alloy hydrolysis LDH is superior to conventional co-precipitation LDH in terms of purity, crystallinity and specific surface area. Mg-Al alloy are of advantages as compared to other Al-based alloys for on-board hydrogen generation as the hydrolysis produces LDH, which has found many applications, including chemical catalysis and water treatment and purification.

Acknowledgements

The authors greatly appreciate the support from the Natural Science Foundation of Beijing Municipality (No. 2182050), the National Natural Science Foundation of China (No. 21506010), China Major Science and Technology Program for Water Pollution Control and Treatment (2018ZX07109-002).

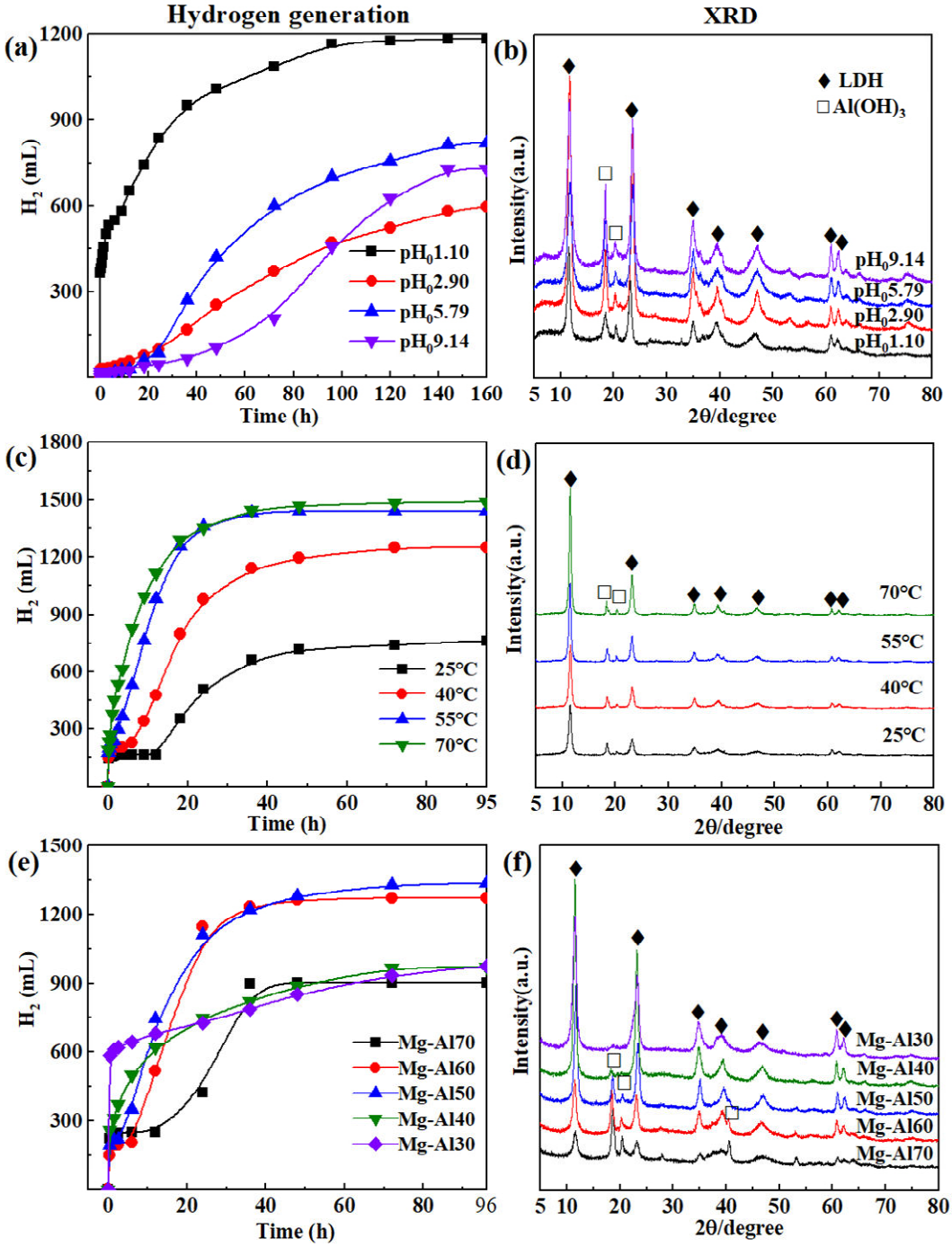


Figure 1. Hydrogen generation and XRD characterization of hydrolysis products. (a, b) effect of initial pH, Mg-Al50, 45°C; (c, d) effect of reaction temperature, Mg-Al50, initial pH=0.93; (e, f) effect of Mg/Al ratio, initial pH=0.98, 45°C. 1.5 g alloy, 80-200 meshes, 150 mL solution.

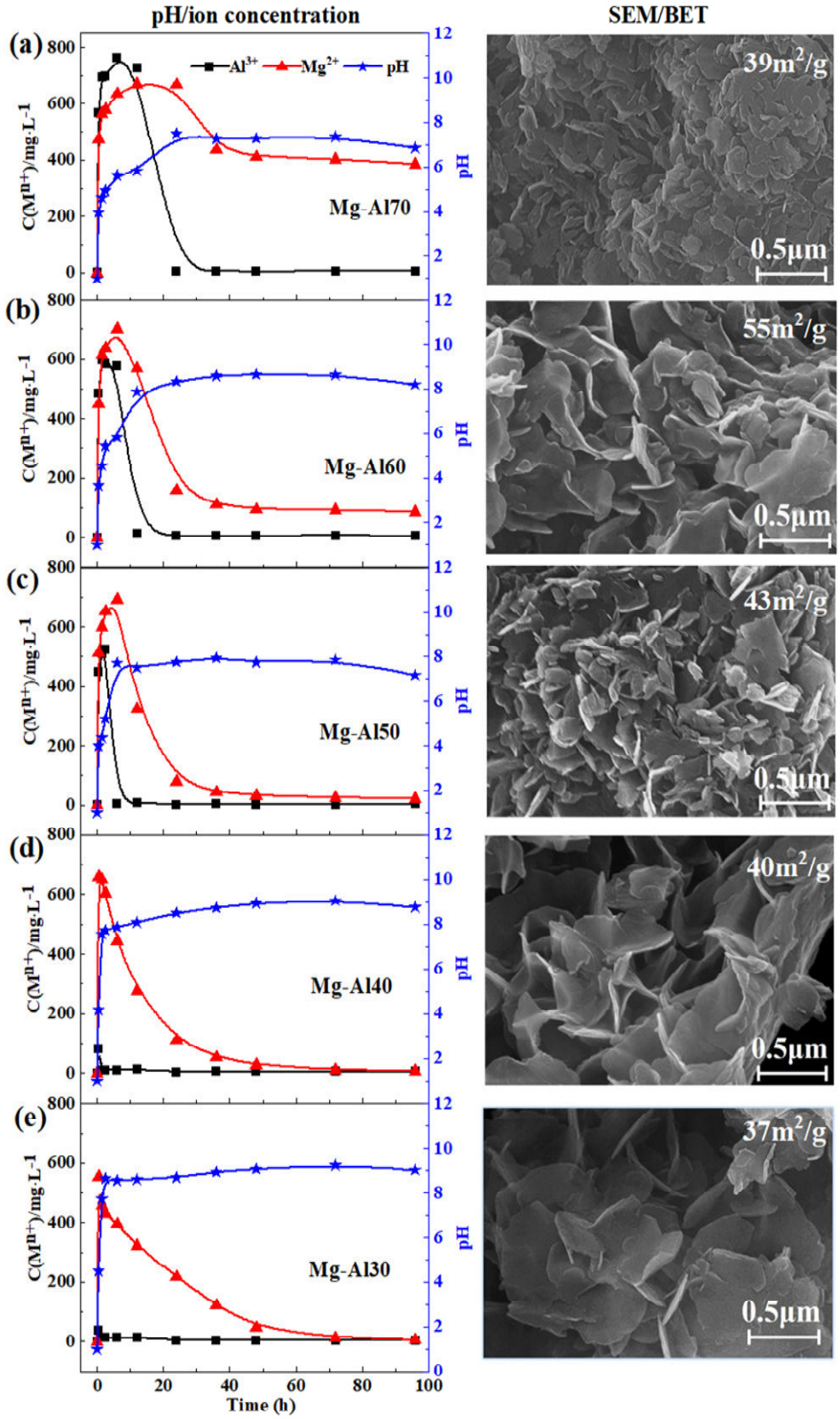


Figure 2. Mg and Al ion concentration and pH profile during the hydrolysis of Mg-Al alloys with different Al concentrations (30-70%) and SEM and BET characterization of the hydrolysis products. (a) Mg-Al70, (b) Mg-Al60, (c) Mg-Al50, (d) Mg-Al40, (e) Mg-Al30. Reaction temperature 45 °C, initial pH 0.98.

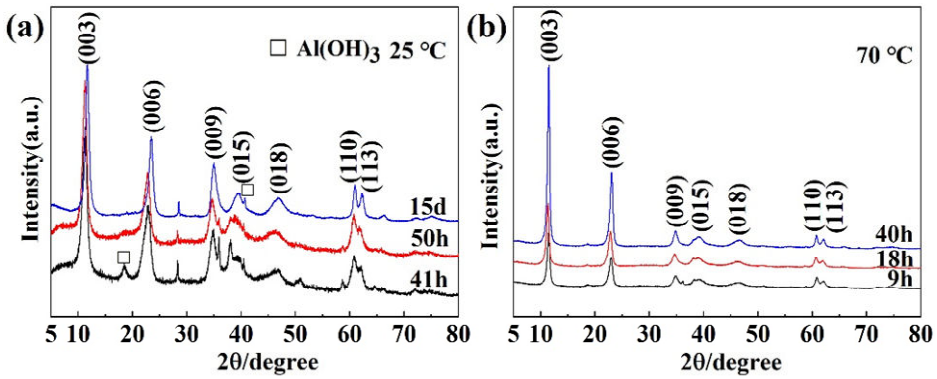


Figure 3. XRD characterization of the Mg-Al30 hydrolysis products under different reaction temperature and time. (a) 25°C; (b) 70°C. Initial pH = 1.0.

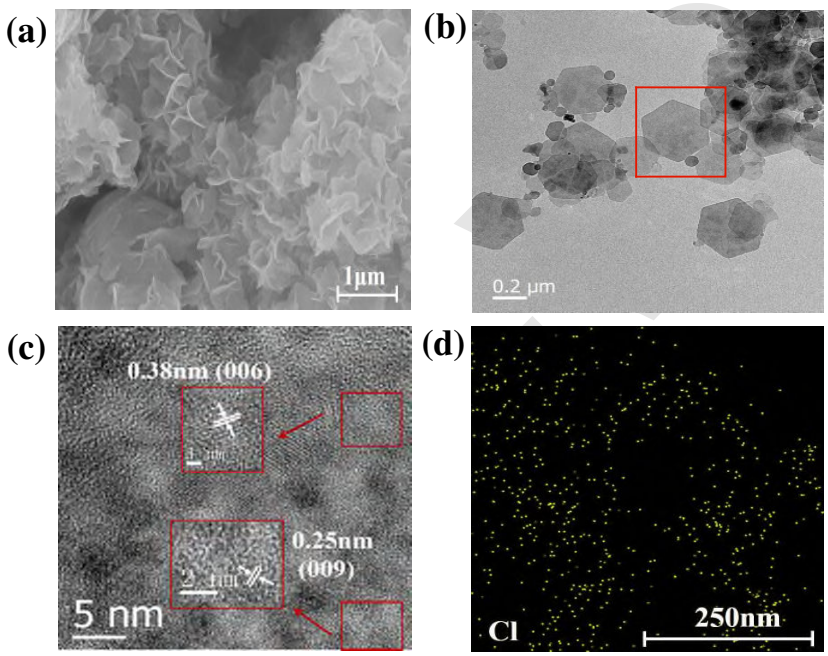


Figure 4. Characterization of Mg-Al alloy hydrolysis LDH. (a) SEM, (b) TEM, (c) HRTEM, (d) Cl-mapping. Conditions: Mg-Al30 (80-200 meshes), 70 °C, initial pH=1.0, t=40 h.

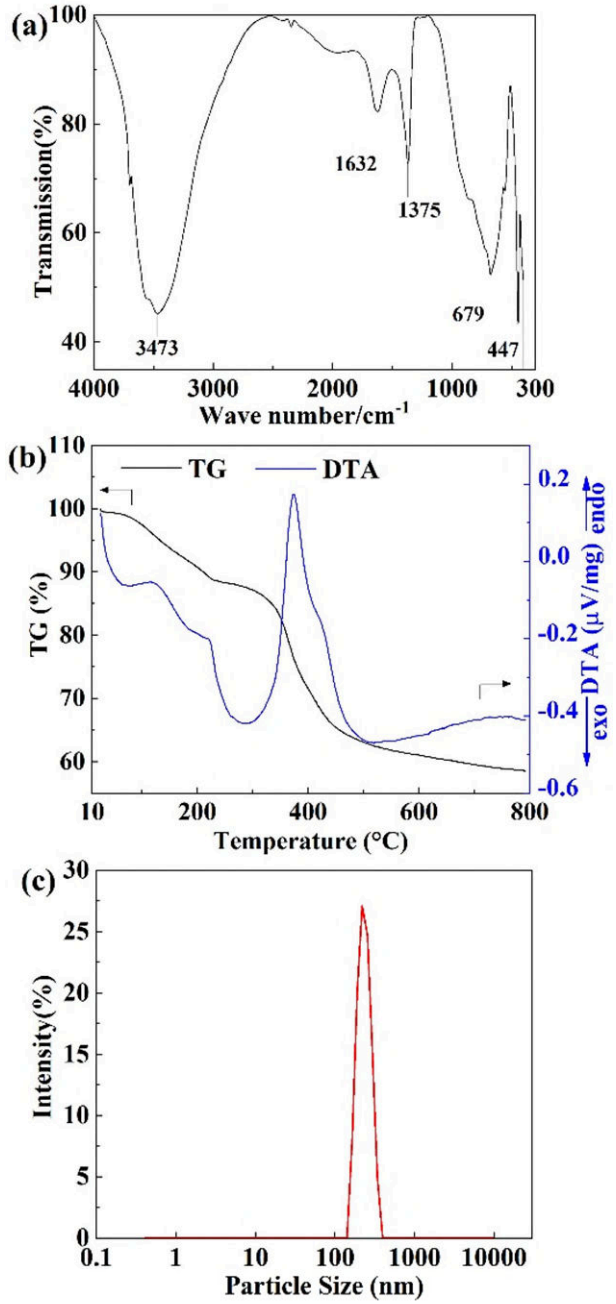


Figure 5. Characterization of Mg-Al alloy hydrolysis LDH. (a) FT-IR, (b) TG-DTA, (c) Particle size.

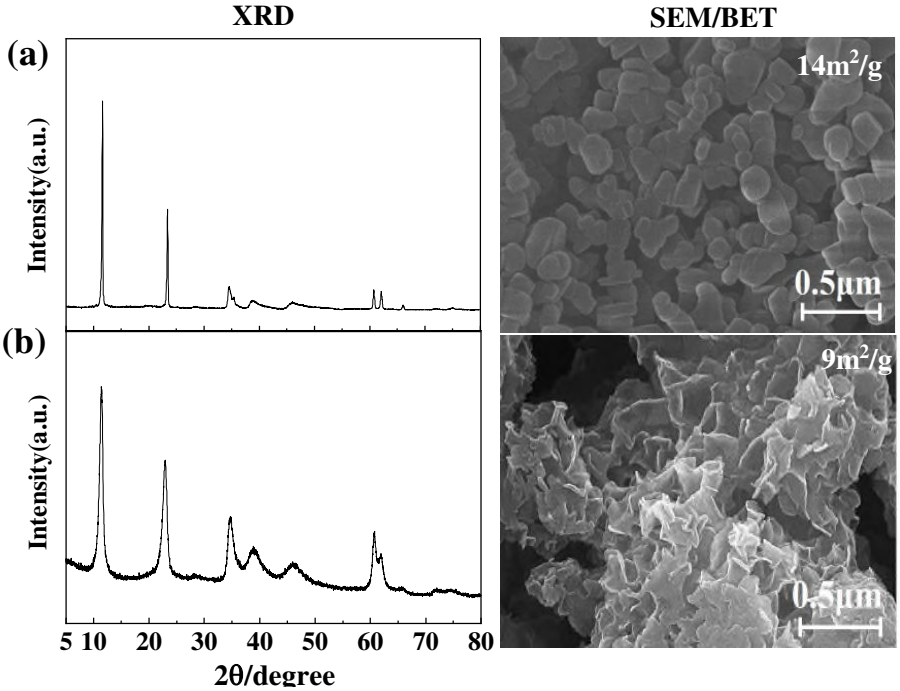


Figure 6. XRD and SEM characterization of (a) commercial and (b) co-precipitation LDH samples (70 °C, 36 h).

Table. 1 Cell parameters, crystallite size and quality of LDH samples

Synthesis Methods	a = 2 d110 (Å)	c = 3 d003 (Å)	E = d003 - 4.8* (Å)	Mg^{2+}/Al^{3+} molar ratio	Average crystallite size# (nm)	BET (m^2/g)	Crystalli-nity (%)	Purity$^{\xi}$ (%)	Refere-nces
Mg-Al alloy hydrolysis	3.046	22.772	2.791	2.20	16	55	92.16%	98.49%	This work
Commercial	10.558	22.710	2.770	2.26	34	14	67.20%	90.66%	This work
Coprecipitation	3.054	23.400	3.000	2.21	24	9	56.64%	95.18%	This work
Coprecipitation	3.042	22.800	3.123	1.69	30	-	-	-	[54]
Coprecipitation	3.042	22.764	2.488	1.92	18	-	-	-	[55]

Notes: * E is the thickness of the lamellar space; 4.8, is the thickness of the brucite layer; # Values calculated from the Scherrer equation; $^{\xi}$ Defined as the percentage of Mg-Al LDH phase to the total content [LDH, $Mg(OH)_2$ and $Al(OH)_3$].

References

[1] X. B. Xie, C. Ni, B. L. Wang, Y. P. Zhang, X. J. Zhao, L. Liu, B. Wang, W. Du, *J. Alloys Compd.*, **2020**, *816,* 152634. http://dx.doi.org/ARTN15263410.1016/j.jallcom.2019.152634

[2] D. E. Balk, *Death Studies*, **2005**, *29 (2),* 179-184. http://dx.doi.org/10.1080/07481180590906200

[3] R. Hardian, C. Pistidda, A. L. Chaudhary, G. Capurso, G. Gizer, H. Cao, C. Milanese, A. Girella, A. Santoru, D. Yigit, H. Dieringa, K. U. Kainer, T. Klassen, M. Dornheim, *Int. J. Hydrogen Energy*, **2018**, *43 (34),* 16738-16748. http://dx.doi.org/10.1016/j.ijhydene.2017.12.014

[4] A. M. Abdalla, S. Hossain, O. B. Nisfindy, A. T. Azad, M. Dawood, A. K. Azad, *Energy Convers. Manage.*, **2018**, *165 (JUN.),* 602-627. http://dx.doi.org/10.1016/j.enconman.2018.03.088

[5] H. Y. Lian, J. L. Liu, X. S. Li, X. B. Zhu, A. Z. Weber, A. M. Zhu, *Chem. Eng. J.*, **2019**, *369,* 245-252. http://dx.doi.org/10.1016/j.cej.2019.03.069

[6] S. Santra, D. Das, N. S. Das, K. K. Nanda, *Chemical Science*, **2017**, *8 (4),* 2994-3001. http://dx.doi.org/10.1039/c7sc00162b

[7] L. Schlapbach, A. Zuttel, *Nature*, **2001**, *414 (6861),* 353-358. http://dx.doi.org/10.1038/35104634

[8] S. Elitzur, V. Rosenband, A. Gany, *Int. J. Hydrogen Energy*, **2017**, *42 (19),* 14003-14009. http://dx.doi.org/10.1016/j.ijhydene.2017.02.037

[9] M. Q. Fan, L. X. Sun, F. Xu, *Energy*, **2010**, *35 (7),* 2922-2926. http://dx.doi.org/10.1016/j.energy.2010.03.023

[10] *Fuel and Energy Abstracts*, **1999**, *40 (6),* 411. http://dx.doi.org/10.1016/s0140-6701(99)99117-8

[11] K. S. Eom, J. Y. Kwon, M. J. Kim, H. S. Kwon, *J. Mater. Chem.*, **2011**, *21 (34),* 13047. http://dx.doi.org/10.1039/c1jm11329a

[12] Y. Y. Jia, J. Shen, H. X. Meng, Y. M. Dong, Y. J. Chai, N. Wang, *J. Alloys Compd.*, **2014**, *588,* 259-264. http://dx.doi.org/10.1016/j.jallcom.2013.11.058

[13] R. Padash, A. H. Jafari, E. Jamalizadeh, *Anti-Corros. Methods Mater.*, **2018**, *65 (4),* 350-360. http://dx.doi.org/10.1108/Acmm-04-2017-1785

[14] H. B. Dai, G. L. Ma, H. J. Xia, P. Wang, *Energy Environ. Sci.*, **2011**, *4 (6),* 2206-2212. http://dx.doi.org/10.1039/c1ee00014d

[15] D. X. Qiao, Y. P. Lu, Z. Y. Tang, X. S. Fan, T. M. Wang, T. J. Li, P. K. Liaw, *Int. J. Hydrogen Energy*, **2019**, *44 (7),* 3527-3537. http://dx.doi.org/10.1016/j.ijhydene.2018.12.124

[16] T. Y. Zhang, W. J. Yang, S. S. Zhang, J. H. Zhou, J. Z. Liu, *Energy Sources, Part A*, **2018**, *40 (1),* 9-14. http://dx.doi.org/10.1080/15567036.2017.1315759

[17] Z. Zhao, X. Chen, M. Hao, *Energy*, **2011**, *36 (5),* 2782-2787. http://dx.doi.org/10.1016/j.energy.2011.02.018

[18] M. Kim, K. Eom, J. Kwon, E. Cho, H. Kwon, *J. Power Sources*, **2012**, *217,* 345-350. http://dx.doi.org/10.1016/j.jpowsour.2012.06.008

[19] K. Eom, E. Cho, H. Kwon, *Int. J. Hydrogen Energy*, **2011**, *36 (19),* 12338-12342. http://dx.doi.org/10.1016/j.ijhydene.2011.06.099

[20] X. Y. Chen, Z. W. Zhao, M. M. Hao, D. Z. Wang, *J. Power Sources*, **2013**, *222,* 188-195. http://dx.doi.org/10.1016/j.jpowsour.2012.08.078

[21] S. Al Bacha, M. Zakhour, M. Nakhl, J. L. Bobet, *Int. J. Hydrogen Energy*, **2020**, *45 (11),* 6102-6109. http://dx.doi.org/10.1016/j.ijhydene.2019.12.162

[22] L. Escobar-Alarcon, J. L. Iturbe-Garcia, F. Gonzalez-Zavala, D. A. Solis-Casados, R. Perez-Hernandez, E. Haro-Poniatowski, *Appl. Surf. Sci.*, **2019**, *478,* 189-196. http://dx.doi.org/10.1016/j.apsusc.2019.01.213

[23] A. Irankhah, S. M. S. Fattahi, M. Salem, *Int. J. Hydrogen Energy*, **2018**, *43 (33),* 15739-15748. http://dx.doi.org/10.1016/j.ijhydene.2018.07.014

[24] M. Mon, R. Bruno, J. Ferrando-Soria, D. Armentano, E. Pardo, *Journal Of Materials Chemistry A*, **2018**, *6 (12),* 4912-4947. http://dx.doi.org/10.1039/c8ta00264a

[25] A. R. Sotiles, L. M. Baika, M. T. Grassi, F. Wypych, *J. Am. Chem. Soc.*, **2018**, *141 (1),* 531-540. http://dx.doi.org/10.1021/jacs.8b11389

[26] Z. Z. Yang, F. H. Wang, C. Zhang, G. M. Zeng, X. F. Tan, Z. G. Yu, Y. Zhong, H. Wang, F. Cui, *Rsc Advances*, **2016**, *6 (83),* 79415-79436. http://dx.doi.org/10.1039/c6ra12727d

[27] M. Zubair, M. Daud, G. McKay, F. Shehzad, M. A. Al-Harthi, *Appl. Clay Sci.*, **2017**, *143 (JUL.),* 279-292. http://dx.doi.org/10.1016/j.clay.2017.04.002
[28] K. Shimizu, J. Shibata, A. Satsuma, *J. Catal.*, **2006**, *239 (2),* 402-409. http://dx.doi.org/10.1016/j.jcat.2006.02.011
[29] S. A. Kondrat, P. J. Smith, P. P. Wells, P. A. Chater, J. H. Carter, D. J. Morgan, E. M. Fiordaliso, J. B. Wagner, T. E. Davies, L. Lu, J. K. Bartley, S. H. Taylor, M. S. Spencer, C. J. Kiely, G. J. Kelly, C. W. Park, M. J. Rosseinsky, G. J. Hutchings, *Nature*, **2016**, *531 (7592),* 83-87. http://dx.doi.org/10.1038/nature16935
[30] N. Chubar, R. Gilmour, V. Gerda, M. Micusik, M. Omastova, K. Heister, P. Man, J. Fraissard, V. Zaitsev, *Adv. Colloid Interface Sci.*, **2017**, *245,* 62-80. http://dx.doi.org/10.1016/j.cis.2017.04.013
[31] E. Conterosito, V. Gianotti, L. Palin, E. Boccaleri, D. Viterbo, M. Milanesio, *Inorg. Chim. Acta*, **2018**, *470,* 36-50. http://dx.doi.org/10.1016/j.ica.2017.08.007
[32] W. Tongamp, Q. Zhang, F. Saito, *Journal of Materials Science*, **2007**, *42 (22),* 9210-9215. http://dx.doi.org/10.1007/s10853-007-1866-5
[33] L. N. Stepanova, O. B. Belskaya, A. V. Vasilevich, T. I. Gulyaeva, N. N. Leont'eva, A. N. Serkova, A. N. Salanov, V. A. Likholobov, *Catal. Today*, **2019**.
[34] M. G. Zeng, X. L. Huo, S. Q. Liu, S. P. Li, X. D. Li, *Appl. Surf. Sci.*, **2014**, *292,* 1059-1066. http://dx.doi.org/10.1016/j.apsusc.2013.12.093
[35] Y. D. G. Edañol, J. A. O. Poblador, T. J. E. Talusan, L. M. Payawan, *Materials Today: Proceedings*, **2020**.
[36] R. Pourfaraj, S. J. Fatemi, S. Y. Kazemi, P. Biparva, *J. Colloid Interface Sci.*, **2017**, *508,* 65-74. http://dx.doi.org/https://doi.org/10.1016/j.jcis.2017.07.101
[37] H. Liu, F. Yang, B. Yang, Q. Zhang, Y. Chai, N. Wang, *Catal. Today*, **2018**, *318,* 52-58. http://dx.doi.org/10.1016/j.cattod.2018.03.030
[38] M. Fan, F. Xu, L. Sun, *Int. J. Hydrogen Energy*, **2007**, *32 (14),* 2809-2815. http://dx.doi.org/10.1016/j.ijhydene.2006.12.020
[39] X. Yue, W. Liu, Z. Chen, Z. Lin, *J. Environ. Sci.*, **2017**, *53,* 16-26. http://dx.doi.org/10.1016/j.jes.2016.01.015
[40] H. Z. Wang, D. Y. C. Leung, M. K. H. Leung, M. Ni, *Renewable Sustainable Energy Rev.*, **2009**, *13 (4),* 845-853. http://dx.doi.org/10.1016/j.rser.2008.02.009
[41] K. Abderrazek, N. F. Srasra, E. Srasra, *J. Chin. Chem. Soc.*, **2017**, *64 (3),* 346-353. http://dx.doi.org/10.1002/jccs.201600258
[42] X. Lv, Z. Chen, Y. Wang, F. Huang, Z. Lin, *ACS Appl. Mater. Interfaces*, **2013**, *5 (21),* 11271-11275. http://dx.doi.org/10.1021/am4035009
[43] G. Zhang, L. Wu, A. Tang, B. Weng, A. Atrens, S. Ma, L. Liu, F. Pan, *RSC Advances*, **2018**, *8 (5),* 2248-2259. http://dx.doi.org/10.1039/c7ra11683g
[44] F. Wang, Z. Guo, *J. Alloys Compd.*, **2018**, *767,* 382-391. http://dx.doi.org/10.1016/j.jallcom.2018.07.086
[45] W. Q. Peng, Z. Q. Lan, W. L. Wei, L. Q. Xu, J. Guo, *Int. J. Hydrogen Energy*, **2016**, *41 (3),* 1759-1765. http://dx.doi.org/10.1016/j.ijhydene.2015.11.138
[46] J. C. Crivello, T. Nobuki, S. Kato, M. Abe, T. Kuji, *J. Alloys Compd.*, **2007**, *446,* 157-161. http://dx.doi.org/10.1016/j.jallcom.2006.12.055
[47] M.-S. Zou, X.-Y. Guo, H.-T. Huang, R.-J. Yang, P. Zhang, *J. Power Sources*, **2012**, *219,* 60-64. http://dx.doi.org/10.1016/j.jpowsour.2012.07.008
[48] Y. Guo, X. L. Cui, Y. G. Li, Q. H. Zhang, H. Z. Wang, *J. Nanosci. Nanotechnol.*, **2016**, *16 (6),* 5653-5661. http://dx.doi.org/10.1166/jnn.2016.11725
[49] M. T. Rahman, T. Kameda, S. Kumagai, T. Yoshioka, *Chemosphere*, **2018**, *203,* 281-290. http://dx.doi.org/10.1016/j.chemosphere.2018.03.166
[50] J. Wang, Y. Wei, J. Yu, *Appl. Clay Sci.*, **2013**, *72,* 37-43. http://dx.doi.org/10.1016/j.clay.2013.01.006
[51] A. A. A. Ahmed, Z. A. Talib, M. Z. bin Hussein, A. Zakaria, *J. Solid State Chem.*, **2012**, *191,* 271-278. http://dx.doi.org/10.1016/j.jssc.2012.03.013
[52] W. Yang, Y. Kim, P. K. T. Liu, M. Sahimi, T. T. Tsotsis, *Chem. Eng. Sci.*, **2002**, *57 (15),* 2945-2953. http://dx.doi.org/10.1016/s0009-2509(02)00185-9

Chemical Engineering & Technology
[53] Z. Karami, M. Jouyandeh, S. Ghiyasi, J. A. Ali, M. R. Ganjali, M. Aghazadeh, M. Maadani, M. Rallini, F. Luzi, L. Torre, D. Puglia, M. R. Saeb, *Prog. Org. Coat.*, **2020***, 139,* 105255. http://dx.doi.org/10.1016/j.porgcoat.2019.105255
[54] Y. Zhao, F. Li, R. Zhang, D. G. Evans, X. Duan, *Chem. Mater.*, **2002***, 14 (10),* 4286-4291. http://dx.doi.org/10.1021/cm020370h
[55] Z. P. Xu, H. C. Zeng, *Chem. Mater.*, **2001***, 13 (12),* 4555-4563. http://dx.doi.org/10.1021/cm010222b

Figure captions

Figure 1. Hydrogen generation and XRD characterization of hydrolysis products. (a, b) effect of initial pH, Mg-Al50, 45°C; (c, d) effect of reaction temperature, Mg-Al50, initial pH=0.93; (e, f) effect of Mg/Al ratio, initial pH=0.98, 45°C. 1.5 g alloy, 80-200 meshes, 150 mL solution.

Figure 2. Mg and Al ion concentration and pH profile during the hydrolysis of Mg-Al alloys with different Al concentrations (30-70%) and SEM and BET characterization of the hydrolysis products. (a) Mg-Al70, (b) Mg-Al60, (c) Mg-Al50, (d) Mg-Al40, (e) Mg-Al30. Reaction temperature 45 °C, initial pH 0.98.

Figure 3. XRD characterization of the Mg-Al30 hydrolysis products under different reaction temperature and time. (a) 25°C; (b) 70°C. Initial pH = 1.0.

Figure 4. Characterization of Mg-Al alloy hydrolysis LDH. (a) SEM, (b) TEM, (c) HRTEM, (d) Cl-mapping. Conditions: Mg-Al30 (80-200 meshes), 70 °C, initial pH=1.0, t=40 h.

Figure 5. Characterization of Mg-Al alloy hydrolysis LDH. (a) FT-IR, (b) TG-DTA, (c) Particle size.

Figure 6. XRD and SEM characterization of (a) commercial and (b) co-precipitation LDH samples (70 °C, 36 h).

Table. 1 Cell parameters, crystallite size and quality of LDH samples

Abbreviations

LDH, layer doubled hydroxide

XRD, X-ray diffraction

SEM, scanning electron microscope

TEM, transmission electron microscope

ICP-OES, inductively coupled plasma optical emission spectrometry

BET, specific surface areas

FT-IR, fourier transform infrared spectrometer

TGA, thermal gravimetric analyzer

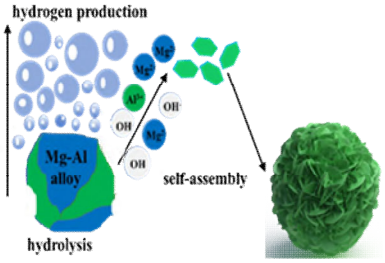
Entry for the Table of Contents

Communication: The hydrolysis of Mg-Al alloy (Mg/Al mass ratio 70/30) generates hydrogen and pure and well-crystallized LDH with an average particle size of 217 nm, crystallite size of 16 nm and a specific surface area of 55 m^2/g

Production of high-purity hydrogen and layered doubled hydroxide by the hydrolysis of Mg-Al alloys

Tong Zheng, Jingqi Zhang, Yang Tang, Pingyu Wan, Qipeng Yuan, Hanjun Hu, Frederic Coulon, Qing Hu, Xiao Jin Yang

Chem. Eng. Technol. **20XX**, *XX (X)*





https://dspace.org/

Production of highpurity hydrogen and layered doubled hydroxide by the hydrolysis of MgAl alloys

Zheng, Tong; Zhang, Jingqi; Tang, Yang; Wan, Pingyu; Yuan, Qipeng ...

2021-02-24
Wiley
https://doi.org/10.1002/ceat.202000590
Zheng T, Zhang J, Tang Y, et al., (2021) Production of highpurity hydrogen and layered doubled hydroxide by the hydrolysis of MgAl alloys. Chemical Engineering and Technology, Volume 44, Issue 4, April 2021, pp. 1-8

Downloaded from a DSpace repository. https://dspace.org/